脱髄関連プロテアーゼの機能解析

16500212

平成16年度～平成17年度科学研究費補助金

（基盤研究（C））研究成果報告書

平成18年4月

研究代表者　吉　田　成　孝

旭川医科大学医学部教授

はしがき

外傷などによる脊髄損傷はその後の機能的回復が多く望めないため、医学的、社会的にも大きな問題となっている。これは、切断された軸索の再生は中枢神経においてはほとんど生じないという事実によるところが大きい。現在、切断された軸索を再生すべく栄養因子の投与や遺伝子改変の試みがなされ、また、神経回路網再構築のために幹細胞を用いた研究も盛んに行われているが実用化にいたる過程にはまだ解決しなければならない問題も多い。これらの点を考慮すると、脊髄損傷や変性疾患において再生により機能を回復する事に加え、損傷を最小限にとどめ機能温存を図る事が重要になってくると考えられる。

我々はオリゴデンドロサイトが2種のセリンプロテアーゼを発現し、損傷等の傷害時にその発現が増強する事を見出してきた。今回の課題による研究ではこれらのプロテアーゼの機能に迫るために、基質候補の探索と遺伝子ノックアウト動物における表現型解析を行った。

研究組織

研究代表者：吉　田　成　孝（旭川医科大学医学部教授）

研究分担者：寺　山　隆　司（岡山大学歯学部助手）

研究分担者：板　東　良　雄（旭川医科大学医学部助手）

交付決定額（配分額）　　（金額単位：千円）

	直接経費	間接経費	合計
平成１６年度	1,700	0	1,700
平成１７年度	1,200	0	1,200
総計	2,900	0	2,900

研究発表

（１）学会誌等

1. Ishida-Yamamoto, A., Simon, M., Kishibe, M., Miyauchi, Y., Takahashi, H., Yoshida, S., O'Brien, T.J., Serre, G. and Iizuka, H., Epidermal Lamellar Granules are Part of Branched Tubular Structures and Transport Different Cargoes as Distinct Aggregates J. Inv. Dermatol. 150, 843-51, 2004.

2. Terayama R., Bando, Y., Takahashi, T. and Yoshida, S., Differential expression of neuropsin and protease M/neurosin in oligodendrocytes after injury to the spinal cord. Glia 48, 91-101, 2004.

3. Terayama R, Bando Y, Jiang Y-P, Mitrovic B, Yoshida S, Differential expression of protease M/neurosin in oligodendrocytes and their progenitors in an animal model of multiple sclerosis., Neurosci Lett, 382, 82-87, 2005.

4. Terayama R, Bando Y, Yamada M, Yoshida S, Involvement of neuropsin in the pathogenesis of experimental autoimmune encephalomyelitis, Glia 52, 108-118, 2005.

5. Yasoshima, Y, Kai N, Yoshida S, Shiosaka S, Koyama Y, Kayama Y, Kobayashi K, Subthalamic Neurons Coordinate Basal Ganglia Function through Differential Neural Pathways, J Neurosci., 25,7743-7753 2005.

6. Yamada M, Terayama R, Bando Y, Kasai S, Yoshida S, Regeneration of the abdominal postganglionic sympathetic system., Neurosci Res, 54, 261-268, 2006.

（2）口頭発表

1. 寺山隆司、吉田成孝、脊髄損傷によるニューロプシンおよびプロテアーゼMの発現変化、第31回日本脳科学会、宮崎、2004.6.11.

2. Terayama R, Yamada M, Yoshida S, Involvement of neuropsin and protease M/neurosin in the pathogenesis of experimental allergic encephalitis, 16th International Congress of the IFAA, Kyoto, 2004.8.

3. Bando Y, Ito Y, Nagai R, Terayama R, Yoshida S, Expression of serine protease protease M / neurosin in demyelination and remyelination, 16th International Congress of the IFAA, Kyoto, 2004.8.

4. 寺山隆司、多発性硬化症モデルマウスにおけるセリンプロテアーゼの発現変化、第６回ORIGIN神経科学研究会夏のワークショップ、美瑛、2004.9.4.

5. 板東良雄、脱髄におけるneurosinの発現とミエリン代謝、第６回ORIGIN神経科学研究会夏のワークショップ、美瑛、2004.9.4.

6. 板東良雄、伊藤慎治、永井美子、寺山隆司、吉田成孝、脱髄におけるセリンプロテアーゼProtease M/neurosinの発現、第47回日本神経化学大会、大阪、2004.9.22.

7. 寺山隆司、板東良雄、吉田成孝、脱髄性神経変性疾患におけるニューロプシンの関与、日本解剖学会第50回東北・北海道連合支部学術集会、札幌、2005.10.17.

8. Bando Y, Terayama R, Yoshida S, Expression of serine protease M/neurosin in

demyelination and remyelination. 34th Annual Meeting of Society for Neuroscience, San Diego, 2004. 10.

9. 吉田成孝、寺山隆司、板東良雄、Experimental allergic encephalitisにおけるオリゴデンドロサイトによるセリンプロテアーゼの発現、第9回グリア研究会、福岡、2004.11.20.

10. 板東良雄、寺山隆司、吉田成孝、オリゴデンドロサイトにおけるセリンプロテアーゼ、第110回日本解剖学会全国学術集会、富山、2005.3.31.

11. 板東良雄、高草木薫、寺山隆司、柏柳誠、吉田成孝、生体におけるマウス脳梁の伝導特性、第28回日本神経科学大会、横浜、2005.7.26.

12. Yoshida S, Terayama R, Bando Y, Neuropsin promotes oligodendroglial cell death, demyelination and axonal degeneration after injury to the spinal cord. 第48回日本神経化学大会、福岡、2005.9.28.

13. 吉田成孝、寺山隆司、板東良雄、ニューロプシンは脊髄損傷後の脱髄と軸索傷害を促進する、日本解剖学会第51回東北・北海道連合支部学術集会、仙台、2005.10.15.

Introduction

The pathophysiology of spinal cord injury (SCI) involves primary and secondary mechanisms. Following an initial impact after SCI, there is delayed and progressive period of secondary damage that contributes to the loss of sensory and voluntary motor function (Lu *et al.*, 2000; Park *et al.*, 2004). This secondary phase of injury includes ischemia, inflammation, glutamate excitotoxicity, and neuronal or glial cell death. These processes are mediated by changes in the constitution of a variety of extracellular matrix components (Sanes, 1983; Sanes, 1989), growth factors (Mocchetti and Wrathall, 1995), and proteolytic cascades (Krystosek and Seeds, 1981; Monard, 1988; Seeds *et al.*, 1990). Several groups have now demonstrated that oligodendroglial cell death and subsequent demyelination have been shown to be involved in the pathology of the spinal cord following injury (Blight, 2002; Lu *et al.*, 2000; Park *et al.*, 2004; Tator and Fehlings, 1991). Oligodendrocytes extend their processes to myelinate axons in the CNS. Poor myelination of surviving axons may be involved in permanent functional impairments. Oligodendroglial loss and demyelination cause conduction deficits in myelinated axons, that could be treated by improving the function of surviving nerve fibers, even in the absence of regeneration.

Since oligodendrocytes have protease activity, which might contribute to the pathology after SCI (Berlet *et al.*, 1984), the identification and characterization of key enzymatic players may suggest new therapeutic targets to reduce lesion load and promote remyelination. Kallikreins are serine proteases that comprise a recently identified large and closely related 15-member family in human. Mice are reported to carry up to 37 kallikrein genes including homologous genes to newly identified human kallikreins. These kallikreins include both regulatory- and degradative-type proteases, serving a variety of physiological function including regulation of blood pressure, neuronal health, and the inflammatory response (Borgono and Diamandis, 2004; Borgono *et al.*, 2004; Diamandis *et al.*, 2004; Olsson and Lundwall, 2002). Neuropsin is a kalliklein-like serine protease whose mRNA is constitutively expressed specifically in the neurons of the limbic system of the adult mouse brain (Chen *et al.*, 1995; Shiosaka and Yoshida, 2000; Yoshida and Shiosaka, 1999). *KLK8* was assigned to the gene for the human analogue (Yoshida *et al.*, 1998; Yousef *et al.*, 2003). Biochemical analysis of recombinant and native neuropsin suggested that it is an

extracellular trypsin-type protease with a relatively narrow spectrum of substrates (Shimizu *et al.*, 1998). Our previous experiments showed that traumatic and excitotoxic injury induced expression of neuropsin mRNA in the area surrounding the lesion in the CNS (Terayama *et al.*, 2004; Tomizawa *et al.*, 1999). Combined in situ hybridization and immunohistochemistry revealed that most of the cells expressing neuropsin mRNA were mature oligodendrocytes (Terayama *et al.*, 2004).

Although upregulation of neuropsin expression after injury to the CNS has been reported, the functional roles of neuropsin are not fully characterized. Using crush injury model, which is a well characterized and consistently reproducible model of spinal cord injury that allows evaluation of both cell biology and behavior (Faulkner *et al.*, 2004; Inman *et al.*, 2002), we examined changes in the expression of neuropsin in wild-type (WT) mice and assessed functional and histopathological changes in neuropsin-deficient (neuropsin$^{-/-}$) mice.

Materials and methods

Mice

Both WT and neuropsin$^{-/-}$ (n = 12 in each strain) mice were bred from heterozygous (neuropsin$^{+/-}$) mice. The heterozygous mice were produced by backcrossing with C57BL/6 mice for 10 generations. Complete loss of neuropsin mRNA was confirmed by cDNA probe covering exon 2-4 including the region of histidine residue essential for proteolytic activity (Hirata *et al.*, 2001; Kirihara *et al.*, 2003). Mice were bred in-house (Division of Laboratory Animal Resources at Asahikawa Medical College), controlled for temperature (20 °C), and maintained with a daily light period of 12 hr. Adult (6- to 8-week-old) mice were used in all experiments. Paralyzed mice were given easy access to food and hand watered at least twice daily.

Surgery

The procedure was approved by the Institutional Committee for Experimental animals. Mice were anesthetized with an intraperitoneal injection of pentobarbital sodium (Nembutal, 40-50 mg/kg). Under a dissecting microscope, a laminectomy was performed at the T10 level to make crush injuries with number 5 Dumont forceps ground down to a tip width of 0.5 mm. Forceps we used in this report were modified with a spacer so that at maximal closure a 0.6 mm space remained (Faulkner *et al.*, 2004). After the wound was sutured, animals were allowed to survive for 1, 4, 7, 10 and 14 days.

Behavioral analysis

WT and neuropsin$^{-/-}$ mice (n = 12 in each strain) were evaluated using two behavioral tasks selected to assess hindlimb function after SCI.

Open field locomotor task. Mice were evaluated in an open field by the same one or two observers blinded to the experimental condition and received a score for movement of each hindlimb using the Basso Beattie Bresnahan (BBB) motor rating scale (Basso *et al.*, 1995). This is a 22-point scale (scores 0-21) that systemically details hindlimb function of joint movement, stepping ability, the degree of fine control of coordinated stepping and trunk stability. Briefly, beginning 5 days prior to SCI, animals were acclimated in an open field arena for 5 min durations. On the day of

SCI, all animals had a score of 21. Test sessions were 4 min in duration and mice were tested at days 1, 4, 7, 10, and 14 post-injury.

Rotorod. To assess balance and ability to coordinate stepping, animals were placed on a single-lane rotorod (Ugo Basile Biological Research Apparatus, Comerio-Varese, Italy) for three trials per session at days 0, 1, 4, 7, 10, and 14 post-injury. The rotorod was set for constant acceleration from 3.0 to 30 rpm over 300 sec, and animals were scored on seconds to fall. Each trial was scored individually and averaged for a final score per session.

Tissue preparation

Another group of mice, different from that for behavioral analysis, were used for histopathological evaluations (n = 30). At days 0, 1, 4, 7 and 14 post-injury, animals (n = 3 per strain at each time point) were re-anesthetized and perfused transcardially with saline followed by 4% paraformaldehyde in 0.1 M phosphate buffer (PB, pH 7.4). The spinal cord including the lesion was removed, postfixed overnight in the same fixative, and then immersed in 30% sucrose in 0.1 M PB for 1-2 days. The spinal cord was then frozen in powdered dry ice, embedded in Tissue-Tek (Miles, Elkhart, IN) optimal cutting temperature compound, and stored at –80 °C prior to use. Frozen 14 μm transverse sections of the spinal cord were cut on a cryostat and mounted onto silane-coated slides. Sections were processed for detection of multiple markers to find the differences between WT and neuropsin$^{-/-}$ mice after SCI.

In situ hybridization

In situ hybridization was performed using digoxigenin (DIG, Roche Molecular Biochemicals, Mannheim, Germany)-labeled cRNA probe for neuropsin mRNA. The method used for in situ hybridization was described in previous papers (Chen *et al.*, 1998; Terayama *et al.*, 2004; Yoshida *et al.*, 1994). In brief, slide-mounted sections were postfixed in 4% formaldehyde in 0.1 M PB, then in 0.1 M PB, and incubated in 10 μg/ml of proteinase K, 50 mM Tris-HCl (pH 7.5), and 5 mM EDTA (pH 8.0) for 5 min at RT, followed by 0.25% acetic anhydrate in 0.1 M triethanolamine (pH 8.0) for 10 min at RT, and finally washed in 0.1 M PB. The sections were dehydrated and defatted in graded alcohol solutions and chloroform, respectively and air-dried before application of

the hybridization buffer containing 50% deionized formamide, 10% dextran sulfate, 0.2% sarcosyl, 0.5 mg/ml of yeast tRNA (Sigma, St Louis, MO), 0.2 mg/ml of denatured salmon sperm DNA (Sigma), and 1× Denhardt's solution (Sigma). Prehybridization was carried out at 55 °C for 1 h with hybridization buffer. Hybridization was performed overnight at 55 °C in a humidified chamber with hybridization buffer containing 10 ng/100 μl of the DIG-labeled cRNA probe. The hybridized sections were washed in 4× standard saline citrate (SSC) buffer (pH 7.4) for 20 min and then in 50% formamide/4× SSC buffer at 60 °C for 30 min. Excess probes were removed with 2μg/ml of RNase A in 10 mM Tris-HCl, 1mM EDTA, and 0.5 M NaCl. Sections were equilibrated with buffer 1 (100 mM Tris-HCl and 150 mM NaCl, pH 7.5), then incubated in buffer 2 (1 % Roche blocking reagent, 100 mM maleic acid, and 150 mM NaCl) at RT for 1 h and incubated with alkaline phosphatase-anti-digoxygenin antibody (Roche Molecular Biochemicals) at a dilution of 1:500 in buffer 2 for 1 h. Sections were washed in buffer 1, equilibrated in buffer 3 (100 mM Tris-HCl, 100 mM NaCl, and 50 mM $MgCl_2$, pH 9.5) and developed for 48 h in the dark with 10% polyvinyl alcohol in buffer 3 containing 3.75 μl/ml of 5-bromo-4-chloro-3-indolyl phosphate (BCIP, Roche Molecular Biochemicals) and 5 μl/ml of nitroblue tetrazolium (NBT, Roche Molecular Biochemicals). Development was stopped by washing with buffer 4 (10 mM Tris-HCl and 1 mM EDTA, pH 8.0). The slides were then coverslipped with 50% glycerol in buffer 4. The specificity of the hybridization signal was verified by comparing adjacent sections hybridized with antisense and sense probes of comparable specific activity.

In situ detection of DNA fragmentation (TUNEL)

Terminal deoxynucleotidyl transferase (TdT)-mediated deoxyuridine triphosphate (dUTP)-fluorescein nick end labeling (TUNEL) was performed for the detection of fragmented DNA. The sections were incubated in tailing buffer containing 0.1 mM ATP, 0.05 mM fluorescein 12-dUTP and 25 U/μl terminal deoxynucleotidyl transferase for 60 min at 37 °C. The sections were counter-stained with Hoechst 33342. Some sections were further processed for immunofluorescence labeling with cell-specific markers as follows: mouse monoclonal anti-glial fibrillary acidic protein (GFAP, Sigma; 1:5,000) to identify astrocytes; mouse monoclonal anti-2', 3'-cyclic nucleotide

3'-phosphodiesterase (CNPase, Sigma; 1:2,000) to identify mature oligodendrocytes; mouse monoclonal anti-microtubule-associated protein 2 (MAP2, Sigma; 1:1,000) to identify neurons; rat monoclonal anti-F4/80 (BMA Biomedical AG, Augst, Switzerland; 1:500) to identify macrophages and microglial cells. The number of TUNEL-positive cells in five randomly selected sections within 400 μm rostral and caudal to the epicenter was counted at each survival time point. The data from three individual experiments were represented as the mean number of cells ± SEM and used for statistical analysis (analysis of variance [ANOVA] with post hoc Fisher's protected least significant differences [PLSD] test and Student's *t* test).

Immunohistochemistry

The sections were immersed in PBS containing 1% Triton X-100 and 0.3% hydrogen peroxide for 1 h. Non-specific antibody binding was blocked with 3 % normal goat serum in PBS containing 2% BSA for 1 h. Subsequently, sections were incubated overnight with monoclonal antibody against CNPase at a dilution of 1:2,000 or non-phosphorylated neurofilament-H (SMI 32; Sternberger Monoclonal, Lutherville, Maryland) at a dilution of 1:5,000. After being washed, sections were incubated with biotinylated goat anti-mouse IgG (Vectastain Elite ABC Kit, Vector Laboratories, Burlingame, CA; 1:200) in 2% BSA in PBS. This was followed by incubation with streptavidine-horseradish peroxidase (Vectastain Elite ABC Kit, Vector Laboratories) and visualization with 3,3' -diaminobenzidine (DAB). The primary antibody was omitted for negative controls. The number of CNPase-immunoreactive cells in the white matter of five randomly selected sections within 400 μm rostral and caudal to the epicenter was counted at each survival time point. The data from three individual experiments were represented as the mean number of cells ± SEM and used for statistical analysis (Student' s *t* test).

Anterograde tract tracing with biotinylated dextran amine (BDA)

To investigate the differences in axonal degeneration between WT and neuropsin$^{-/-}$ mice after SCI, three animals in each strain with or without SCI were gently injected with 10% solution of BDA (MW 10,000; Molecular Probes) into the sensorimotor cortex using a 30 G needle connected to a 1 μl Hamilton syringe (#86200,

Hamilton Company, Reno, NV) at the day of SCI. Three injections (0.3 μl each) were made at 1.0 mm lateral to the midline at 0.0, 0.5, 1.0 mm posterior to bregma, and at depth of 0.5 mm from the cortical surface. The animals were perfused with 4% paraformaldehyde in 0.1 M PB 14 days after SCI. After cryoprotection, frozen spinal cord sections were serially cut at 20 μm in a horizontal plane and mounted onto silane-coated slides. Sections were washed in PBS with 0.3% hydrogen peroxide for 1 h, and then incubated overnight with streptavidine-horseradish peroxidase (Vectastain Elite ABC Kit, Vector Laboratories) and visualization with DAB. The number of CST fibers 1.0 mm rostral and caudal to the lesion epicenter was counted at least 5 sections within 100-300 μm dorsal to the central canal. The data from three individual experiments were represented as the mean number of fibers per section and used for statistical analysis (Student' s *t* test).

Real-time quantitative PCR

After postoperative periods of 0, 1, 4, 7, and 14 days, another group of mice (n = 30) were given a lethal dose of anesthetic (100 mg/kg), a laminectomy was performed to expose the spinal cord, and a 4 mm rostrally-caudally oriented section of the spinal cord, centered on the lesion site, was quickly dissected. Total RNA was extracted using TRIzol reagent (Invitrogen Life Technologies, Carlsbad, CA). The first strand cDNA was synthesized with AMV reverse transcriptase (Promega, Madison, WI) at 42 °C for 1 h. The cDNA was diluted a hundred-fold prior to PCR amplification. The LightCycler rapid thermal cycler system (Roche Diagnostics, Penzberg, Germany) was used according to the manufacture' s instructions. Reactions were performed in a 20 μl volume with 0.5 μM primers and $MgCl_2$ concentration optimized between 2-5 mM. Deoxynucleotides, Taq DNA polymerase, and buffer were included in the LightCycler-DNA Master SYBR Green I mix (Roche Diagnostics). PCR was performed under the following conditions: initial denaturation for 10 min at 95° C, 40 cycles of denaturation for 0 s at 95° C, annealing for 5 s at 56-57° C, and enzymatic chain extension for 10 s at 72° C. Each PCR assay included a negative control consisting of H_2O without any template DNA to monitor for possible contamination. To confirm amplification specificity the PCR products from each primer pairs were subjected to a melting

curve analysis and subsequent agarose gel electrophoresis. The PCR primers were designed according to published sequences of neuropsin, CCCACTGCAAAAAACAGAAG (sense); TGTCAGCTCCATTGCTGCT (antisense) and myelin basic protein (MBP), AGCTCTGGTCTTTCTTGCAG (sense); CCCCGTGGTAGGAATATTACATAAC (antisense). Glyceraldehyde phosphate dehydrogenase (GAPDH) mRNA was used as an internal control: CGGGAAGCCCATCACCATCA (sense); GAGGGGCCATCCACAGTCTT (antisense). All primers were synthesized by Genosys (Sigma).

The quantification data were analyzed with the LightCycler analysis software. A serially diluted cDNA from control mouse spinal cord was used for standard. The level of each specific cDNA was quantified in the exponential phase of the PCR amplification and normalized with the level of GAPDH mRNA expression in each individual sample. The raw data from three individual experiments were used for statistical analysis (ANOVA with post hoc Fisher's PLSD test and Student's *t* test).

The sections and primary OLGs were stained with rabbit polyclonal anti-protease M/neurosin antibody (1:500), mouse monoclonal anti-GST-p antibody (BD Biosci., Tokyo, Japan; 1:125) for mature OLGs, anti-MBP antibody (Chemicon, 1:1000) or anti-2'-3'-cyclic nucleotide 3'-phosphodiesterase antibody (CNPase; Chemicon, 1:1000). The sections or cells were incubated overnight with either primary antibody at RT. Alexa-594 and Alexa-488 (Molecular Probes, Eugene, OR)-conjugated secondary antibodies were used to visualize primary antibody binding. Sections or cells were analyzed with a fluorescence microscope (ECLIPSE 80i; Nikon, Japan). In some experiments, the cells were also stained with 4',6-diamidine-2-phenylindole dihydrochloride (DAPI; Sigma) to display nuclei. Some sections and cultured OLGs were subjected to terminal deoxynucleotidyltransferase-mediated dUTP-biotin neck-end labeling (TUNEL) assay after immunostaining with anti-GST-p antibody. The sections were stained with a DEADend Fluorometric TUNEL system following the manufacturer's protocol (Promega, Madison, WI).

Results

Changes in the expression of neuropsin mRNA after injury to the spinal cord

We first examined neuropsin mRNA expression within unlesioned and lesioned spinal cord of WT mice. The distribution of mRNA encoding neuropsin was determined by in situ hybridization using specific probe. There was an increase in the expression of neuropsin mRNA after crush SCI (Fig. 1). Within untreated control animals, neuropsin mRNA was observed in a small number of cells in the gray but not white matter of the spinal cord (Fig. 1A). After SCI, neuropsin mRNA was induced in the white matter immediately adjacent to the lesion. This induction was observed at days 1-14 post-injury, peaking at day 4 (Fig. 1B,C). The RT-PCR analysis using a real time LightCycler system confirmed that the expression of mRNA encoding neuropsin was upregulated after SCI (Fig. 1D). At 1-14 days post-injury, neuropsin exhibited a significant increase in mRNA expression, peaking at 4 days (days 1 and 14, $P < 0.05$; days 7, $P < 0.01$; days 4, $P < 0.001$).

Improved recovery of hindlimb function in neuropsin$^{-/-}$ mice

To examine the role of neuropsin after SCI, WT and neuropsin$^{-/-}$ mice were evaluated using two behavioral tasks including open-field locomotor BBB score and rotorod. As shown in Figure 2, neuropsin$^{-/-}$ mice showed a significant improved recovery from hindlimb impairments compared to WT mice. Both WT and neuropsin$^{-/-}$ mice exhibited the initial impairments of motor function on open-field locomotor performance showing no voluntary hindlimb movement or slight voluntary movement at day 1 after SCI, and there was no significant difference between WT and neuropsin$^{-/-}$ mice ($P = 0.389$). These were followed by a gradual recovery over 14-day period after SCI. At days 10 and 14, the hindlimb function in both strains of mice showed some recovery, but scores in neuropsin$^{-/-}$ mice were significantly higher than WT mice ($P < 0.05$; Fig. 2A). Similarly, performance on rotorod dramatically impaired at day 1 after SCI followed by a gradual recovery over 14 days. At days 10 and 14, neuropsin$^{-/-}$ mice showed significantly higher rotorod performance compared to WT mice ($P < 0.05$; Fig. 2B). These results indicate that neuropsin may contribute to the inhibition of functional recovery from SCI.

Attenuated demyelination in neuropsin$^{-/-}$ mice after injury

The results of immunohistochemistry for MBP and RT-PCR for MBP mRNA demonstrated that demyelination was attenuated in neuropsin$^{-/-}$ mice (Fig. 3). Extensive defects in MBP immunoreactivity in the spinal cord white matter of WT mice were observed at day 14 after SCI, whereas for the neuropsin$^{-/-}$ mice, relatively minimal demyelination was observed (Fig. 3A-D). The RT-PCR analysis using a real time LightCycler system demonstrated changes in the expression of MBP mRNA after SCI. A rapid and dramatic downregulation of MBP mRNA expression was observed at days 1-14 in WT mice. In neuropsin$^{-/-}$ mice, a decrease in the expression of MBP mRNA was also found but it was significantly less extensive ($P < 0.05$; Fig. 3E). These results indicate that neuropsin is involved in the onset and progression of demyelination.

Attenuated oligodendroglial cell death in neuropsin$^{-/-}$ mice after injury

Spinal cord sections from WT and neuropsin$^{-/-}$ mice at different time points after SCI were processed for TUNEL to detect fragmented DNA. The appearance of TUNEL-positive cells was attenuated in neuropsin$^{-/-}$ mice as compared to WT mice (Fig. 4). Although both strains of mice showed significant number of TUNEL-positive cells after SCI, the number of positive cells was significantly smaller in neuropsin$^{-/-}$ mice than WT mice at days 1 and 4 ($P < 0.05$; Fig. 4A, B). At days 7 and 14, the number of TUNEL-positive cells was decreased to the control level in both strains of mice (Fig. 4A, B). To determine the identity of the TUNEL-positive cells in the spinal cord after injury, some sections from WT mice were further processed for immunofluorescence labeling with cell-specific markers. Most of the cells positive for TUNEL in the white matter immediately adjacent to the lesion showed immunoreactivity for CNPase. By contrast, these cells did not colocalize with immunoreactivity for GFAP, NG2, MAP-2 and F4/80 (data not shown). These results indicate that mature oligodendrocytes suffer from cell death after SCI.

To evaluate the oligodendroglial loss caused by injury, spinal cord sections from WT and neuropsin$^{-/-}$ mice at days 0 and 14 were processed for immunohistochemistry for CNPase. As shown in Figure 5, oligodendroglial loss was attenuated in neuropsin$^{-/-}$ mice at day 14 after injury. A large number of CNPase-positive oligodendrocytes were seen in the white matter of the spinal cord from WT and

neuropsin$^{-/-}$ naïve mice (Fig. 5A, B). At day 14 after injury, the reduction in the number of CNPase-positive cells was prominent in WT mice (Fig. 5C, E). Neuropsin$^{-/-}$ mice also showed the reduction in the number of cells, but it was significantly less extensive and there was a significant difference in the number of positive cells between WT and neuropsin$^{-/-}$ mice at day 14 after SCI ($P < 0.05$; Fig. 5D, E).

Attenuated axonal damage and degeneration in neuropsin$^{-/-}$ mice after injry

The presence of abnormal dephosphorylation of heavy chain neurofilament H (NF-H) has been used to assess axonal damage (Trapp *et al.*, 1998). To evaluate axonal damage in WT and neuropsin$^{-/-}$ mice after SCI, spinal cord sections were processed for immunohistochemistry of dephosphorylated NF-H. As shown in Figure 6A-C, neuropsin$^{-/-}$ mice attenuated accumulation of abnormally dephosphorylated NF-H after SCI. A background level of reactivity was detected in the spinal cords of naive mice (Fig 6A). WT mice had large amounts of dephosphorylated NF-H at day 14 after injury (Fig. 6B). In contrast, neuropsin$^{-/-}$ mice resulted in a less amount of dephosphorylated NF-H as compared with WT mice (Fig. 6C). These results indicate that involvement of neuropsin in the axonal damage after injury.

Axonal degeneration caused by SCI was assessed by anterograde tract tracing with BDA (Fig. 7). SCI resulted in a prominent axonal degeneration of CST fibers indicated by a decrease in density of BDA-labeled fibers caudal to the lesion site at day 14 after injury (Fig. 7D-I). In WT mice, axonal degeneration was observed not only caudal but also rostral to the lesion site (Fig. 7D, E). The number of BDA-labeled fibers 1.0 mm rostral and caudal to the lesion was significantly decreased after SCI in WT mice (Fig. 7J). Neuropsin$^{-/-}$ mice also showed degeneration of CST fibers caudal but not rostral to the lesion site (Fig. 7G-I). The number of labeled fibers caudal to the lesion in neuropsin$^{-/-}$ mice was significantly larger than that in WT mice although a significant reduction after SCI was observed (Fig. 7J).

Discussion

The series of experiments in this study show the potential involvement of neuropsin in the secondary damage after SCI. We demonstrated changes in the expression of neuropsin mRNA after injury in WT mice. In agreement with previous studies, the expression of neuropsin mRNA was increased in the white matter of the spinal cord after injury to the CNS (Terayama *et al.*, 2004; Tomizawa *et al.*, 1999). Extending previous results, our findings demonstrated that neuropsin may promote oligodendroglial death, demyelination and axonal degeneration after SCI. Using mice lacking neuropsin, we examined recovery from the initial impairments of hindlimb function and histopathology after SCI. We found that neuropsin$^{-/-}$ mice exhibit (1) improved recovery of hindlimb function; (2) attenuated demyelination and oligodendroglial cell death; and (3) attenuated axonal damage and degeneration.

Oligodendroglial death is a prominent feature of the secondary degeneration after SCI (Blight, 2002; Lu *et al.*, 2000; Park *et al.*, 2004; Tator and Fehlings, 1991). Glutamatergic excitotoxicity resulting in neuronal death has been well documented in various models of CNS injury (Choi, 1988; Lipton and Rosenberg, 1994). Several lines of evidence has suggested that glutamate excitotoxicity plays a key role not only in neuronal cell death but also in delayed posttraumatic spinal cord white matter degeneration (Agrawal and Fehlings, 1997; Faden and Simon, 1988; Wrathall *et al.*, 1994; Wrathall *et al.*, 1997; Yanase *et al.*, 1995). It has been documented that oligodendrocytes are highly vulnerable to excitotoxic signals mediated by glutamate receptors of the AMPA and kainate classes (Matute *et al.*, 1997; McDonald *et al.*, 1998; Yoshioka *et al.*, 1996). A transient increase in extracellular levels of glutamate following SCI (Farooque *et al.*, 1996; Liu *et al.*, 1991; Liu *et al.*, 1999; McAdoo *et al.*, 1999) has been implicated in mediating secondary injury mechanisms via AMPA and kainate receptors (Agrawal and Fehlings, 1997; Matute *et al.*, 2001; Van Den Bosch and Robberecht, 2000). The possibility of AMPA/kainite receptors as significant contributors to secondary injury mechanisms in SCI is supported by pharmacological studies demonstrating neuroprotective effects both in vivo and in vitro with the application of AMPA/kainate antagonist 2,3-dihydroxy-6-nitro-7-sulfonyl-benzo[*f*]quinoxaline (NBQX) (Agrawal and Fehlings, 1997; Li and Stys, 2000; Rosenberg *et al.*, 1999; Wrathall *et al.*, 1994; Wrathall *et al.*,

1997). Our previous experiments showed that excitotoxic injury caused by injection of kainate into the CNS induced expression of neuropsin mRNA in oligodendrocytes (Tomizawa *et al.*, 1999). Furthermore, it has been shown that the proteolytic activation of neuropsin is induced in a glutamate receptor-dependent manner (Matsumoto-Miyai *et al.*, 2003). The results of the present study demonstrated that SCI induced neuropsin mRNA expression in the white matter and neuropsin$^{-/-}$ mice showed attenuated oligodendroglial death. Data from RT-PCR for MBP mRNA in WT and neuropsin$^{-/-}$ mice also indicate that neuropsin is involved in oligodendroglial death. Thus, both previous and present results suggest that neuropsin is involved, at least in part, in excitotoxic oligodendroglial death mediated by glutamate receptors.

Although neuropsin has been shown to be involved in oligodendroglial death which may cause secondarily demyelination, proteolytic activity of neuropsin can also be considered to mediate demyelination in the pathology of SCI. It has been suggested that myelin has endogenous protease activity with the potential to degrade myelin proteins (Berlet *et al.*, 1984; Chantry *et al.*, 1989; Sato *et al.*, 1982). The in vitro biochemical assay showed that neuropsin is capable of degrading MBP (He *et al.*, 2001). This activity would indicate that neuropsin functions in demyelination through the proteolysis of myelin proteins. The present results from immunohistochemistry for MBP in WT and neuropsin$^{-/-}$ mice also indicate that neuropsin is involved in demyelination.

One of the most striking results in this study was that neuropsin$^{-/-}$ mice showed a significant improved recovery from the initial impairments of hindlimb function. SCI exhibits temporal and spatial range from early neuronal death at the focal lesion site to degeneration of white matter tracts weeks after injury. Degradation of neurofilament and loss of axonal integrity has been reported as early as 15 min after experimental SCI (Banik *et al.*, 1982; Schumacher *et al.*, 1999; Schumacher *et al.*, 2000). The concurrent loss of oligodendrocytes in degenerating axon tracts suggest an intimate relationship between oligodendroglial survival and axonal integrity (Barres *et al.*, 1993; Crowe *et al.*, 1997; Warden *et al.*, 2001). Since oligodendrocytes myelinate several axons simultaneously, the loss of a single cell can influence neighbouring axons. The present study showed that neuropsin$^{-/-}$ mice resulted in a less amount of dephosphorylated NF-H as compared with WT mice after SCI. We also demonstrated

attenuation of axonal degeneration in neuropsin$^{-/-}$ mice at day 14 post-injury. These results suggest that oligodendroglial loss caused by neuropsin activity may involve in axonal damage and degeneration although the causal relationship between oligodendroglial death and axonal degeneration remain to be clarified.

In summary, we showed here the involvement of neuropsin in the secondary injury mechanisms after SCI. Neuropsin may contribute to the onset and progression of demyelination, oligodendroglial cell death, and axonal degeneration. Our results suggest that attenuation of neuropsin activity could prove beneficial in combination with the existing therapeutic management of SCI.

References

Agrawal SK, Fehlings MG (1997) Role of NMDA and non-NMDA ionotropic glutamate receptors in traumatic spinal cord axonal injury. J Neurosci 17: 1055-63.

Banik NL, Hogan EL, Powers JM, Whetstine LJ (1982) Degradation of cytoskeletal proteins in experimental spinal cord injury. Neurochem Res 7: 1465-75.

Barres BA, Jacobson MD, Schmid R, Sendtner M, Raff MC (1993) Does oligodendrocyte survival depend on axons? Curr Biol 3: 489-97.

Basso DM, Beattie MS, Bresnahan JC (1995) A sensitive and reliable locomotor rating scale for open field testing in rats. J Neurotrauma 12: 1-21.

Berlet HH, Ilzenhofer H, Schulz G (1984) Cleavage of myelin basic protein by neutral protease activity of human white matter and myelin. J Neurochem 43: 627-33.

Blight AR (2002) Miracles and molecules--progress in spinal cord repair. Nat Neurosci 5: 1051-4.

Borgono CA, Diamandis EP (2004) The emerging roles of human tissue kallikreins in cancer. Nat Rev Cancer 4: 876-90.

Borgono CA, Michael IP, Diamandis EP (2004) Human tissue kallikreins: physiologic roles and applications in cancer. Mol Cancer Res 2: 257-80.

Chantry A, Gregson NA, Glynn P (1989) A novel metalloproteinase associated with brain myelin membranes. Isolation and characterization. J Biol Chem 264: 21603-7.

Chen ZL, Momota Y, Kato K, Taniguchi M, Inoue N, Shiosaka S, et al. (1998) Expression of neuropsin mRNA in the mouse embryo and the pregnant uterus. J

Histochem Cytochem 46: 313-20.

Chen ZL, Yoshida S, Kato K, Momota Y, Suzuki J, Tanaka T, et al. (1995) Expression and activity-dependent changes of a novel limbic-serine protease gene in the hippocampus. J Neurosci 15: 5088-97.

Choi DW (1988) Glutamate neurotoxicity and diseases of the nervous system. Neuron 1: 623-34.

Crowe MJ, Bresnahan JC, Shuman SL, Masters JN, Beattie MS (1997) Apoptosis and delayed degeneration after spinal cord injury in rats and monkeys. Nat Med 3: 73-6.

Diamandis EP, Yousef GM, Olsson AY (2004) An update on human and mouse glandular kallikreins. Clin Biochem 37: 258-60.

Faden AI, Simon RP (1988) A potential role for excitotoxins in the pathophysiology of spinal cord injury. Ann Neurol 23: 623-6.

Farooque M, Hillered L, Holtz A, Olsson Y (1996) Changes of extracellular levels of amino acids after graded compression trauma to the spinal cord: an experimental study in the rat using microdialysis. J Neurotrauma 13: 537-48.

Faulkner JR, Herrmann JE, Woo MJ, Tansey KE, Doan NB, Sofroniew MV (2004) Reactive astrocytes protect tissue and preserve function after spinal cord injury. J Neurosci 24: 2143-55.

He XP, Shiosaka S, Yoshida S (2001) Expression of neuropsin in oligodendrocytes after injury to the CNS. Neurosci Res 39: 455-62.

Hirata A, Yoshida S, Inoue N, Matsumoto-Miyai K, Ninomiya A, Taniguchi M, et al. (2001) Abnormalities of synapses and neurons in the hippocampus of neuropsin-deficient mice. Mol Cell Neurosci 17: 600-10.

Inman D, Guth L, Steward O (2002) Genetic influences on secondary degeneration and wound healing following spinal cord injury in various strains of mice. J Comp Neurol 451: 225-35.

Kirihara T, Matsumoto-Miyai K, Nakamura Y, Sadayama T, Yoshida S, Shiosaka S (2003) Prolonged recovery of ultraviolet B-irradiated skin in neuropsin (KLK8)-deficient mice. Br J Dermatol 149: 700-6.

Krystosek A, Seeds NW (1981) Plasminogen activator release at the neuronal growth cone. Science 213: 1532-4.

Li S, Stys PK (2000) Mechanisms of ionotropic glutamate receptor-mediated

excitotoxicity in isolated spinal cord white matter. J Neurosci 20: 1190-8.

Lipton SA, Rosenberg PA (1994) Excitatory amino acids as a final common pathway for neurologic disorders. N Engl J Med 330: 613-22.

Liu D, Thangnipon W, McAdoo DJ (1991) Excitatory amino acids rise to toxic levels upon impact injury to the rat spinal cord. Brain Res 547: 344-8.

Liu D, Xu GY, Pan E, McAdoo DJ (1999) Neurotoxicity of glutamate at the concentration released upon spinal cord injury. Neuroscience 93: 1383-9.

Lu J, Ashwell KW, Waite P (2000) Advances in secondary spinal cord injury: role of apoptosis. Spine 25: 1859-66.

Matsumoto-Miyai K, Ninomiya A, Yamasaki H, Tamura H, Nakamura Y, Shiosaka S (2003) NMDA-dependent proteolysis of presynaptic adhesion molecule L1 in the hippocampus by neuropsin. J Neurosci 23: 7727-36.

Matute C, Alberdi E, Domercq M, Perez-Cerda F, Perez-Samartin A, Sanchez-Gomez MV (2001) The link between excitotoxic oligodendroglial death and demyelinating diseases. Trends Neurosci 24: 224-30.

Matute C, Sanchez-Gomez MV, Martinez-Millan L, Miledi R (1997) Glutamate receptor-mediated toxicity in optic nerve oligodendrocytes. Proc Natl Acad Sci U S A 94: 8830-5.

McAdoo DJ, Xu GY, Robak G, Hughes MG (1999) Changes in amino acid concentrations over time and space around an impact injury and their diffusion through the rat spinal cord. Exp Neurol 159: 538-44.

McDonald JW, Althomsons SP, Hyrc KL, Choi DW, Goldberg MP (1998) Oligodendrocytes from forebrain are highly vulnerable to AMPA/kainate receptor-mediated excitotoxicity. Nat Med 4: 291-7.

Mocchetti I, Wrathall JR (1995) Neurotrophic factors in central nervous system trauma. J Neurotrauma 12: 853-70.

Monard D (1988) Cell-derived proteases and protease inhibitors as regulators of neurite outgrowth. Trends Neurosci 11: 541-4.

Olsson AY, Lundwall A (2002) Organization and evolution of the glandular kallikrein locus in Mus musculus. Biochem Biophys Res Commun 299: 305-11.

Park E, Velumian AA, Fehlings MG (2004) The role of excitotoxicity in secondary mechanisms of spinal cord injury: a review with an emphasis on the implications for

white matter degeneration. J Neurotrauma 21: 754-74.

Rosenberg LJ, Teng YD, Wrathall JR (1999) 2,3-Dihydroxy-6-nitro-7-sulfamoyl-benzo(f)quinoxaline reduces glial loss and acute white matter pathology after experimental spinal cord contusion. J Neurosci 19: 464-75.

Sanes JR (1983) Roles of extracellular matrix in neural development. Annu Rev Physiol 45: 581-600.

Sanes JR (1989) Extracellular matrix molecules that influence neural development. Annu Rev Neurosci 12: 491-516.

Sato S, Quarles RH, Brady RO (1982) Susceptibility of the myelin-associated glycoprotein and basic protein to a neutral protease in highly purified myelin from human and rat brain. J Neurochem 39: 97-105.

Schumacher PA, Eubanks JH, Fehlings MG (1999) Increased calpain I-mediated proteolysis, and preferential loss of dephosphorylated NF200, following traumatic spinal cord injury. Neuroscience 91: 733-44.

Schumacher PA, Siman RG, Fehlings MG (2000) Pretreatment with calpain inhibitor CEP-4143 inhibits calpain I activation and cytoskeletal degradation, improves neurological function, and enhances axonal survival after traumatic spinal cord injury. J Neurochem 74: 1646-55.

Seeds NW, Haffke S, Christensen K, Schoonmaker J (1990) Cerebellar granule cell migration involves proteolysis. Adv Exp Med Biol 265: 169-78.

Shimizu C, Yoshida S, Shibata M, Kato K, Momota Y, Matsumoto K, et al. (1998) Characterization of recombinant and brain neuropsin, a plasticity-related serine protease. J Biol Chem 273: 11189-96.

Shiosaka S, Yoshida S (2000) Synaptic microenvironments--structural plasticity, adhesion molecules, proteases and their inhibitors. Neurosci Res 37: 85-9.

Tator CH, Fehlings MG (1991) Review of the secondary injury theory of acute spinal cord trauma with emphasis on vascular mechanisms. J Neurosurg 75: 15-26.

Terayama R, Bando Y, Takahashi T, Yoshida S (2004) Differential expression of neuropsin and protease M/neurosin in oligodendrocytes after injury to the spinal cord. Glia 48: 91-101.

Tomizawa K, He X, Yamanaka H, Shiosaka S, Yoshida S (1999) Injury induces

neuropsin mRNA in the central nervous system. Brain Res 824: 308-11.

Trapp BD, Peterson J, Ransohoff RM, Rudick R, Mork S, Bo L (1998) Axonal transection in the lesions of multiple sclerosis. N Engl J Med 338: 278-85.

Van Den Bosch L, Robberecht W (2000) Different receptors mediate motor neuron death induced by short and long exposures to excitotoxicity. Brain Res Bull 53: 383-8.

Warden P, Bamber NI, Li H, Esposito A, Ahmad KA, Hsu CY, et al. (2001) Delayed glial cell death following wallerian degeneration in white matter tracts after spinal cord dorsal column cordotomy in adult rats. Exp Neurol 168: 213-24.

Wrathall JR, Choiniere D, Teng YD (1994) Dose-dependent reduction of tissue loss and functional impairment after spinal cord trauma with the AMPA/kainate antagonist NBQX. J Neurosci 14: 6598-607.

Wrathall JR, Teng YD, Marriott R (1997) Delayed antagonism of AMPA/kainate receptors reduces long-term functional deficits resulting from spinal cord trauma. Exp Neurol 145: 565-73.

Yanase M, Sakou T, Fukuda T (1995) Role of N-methyl-D-aspartate receptor in acute spinal cord injury. J Neurosurg 83: 884-8.

Yoshida S, Lin LP, Chen ZL, Momota Y, Kato K, Tanaka T, et al. (1994) Basal magnocellular and pontine cholinergic neurons coexpress FGF receptor mRNA. Neurosci Res 20: 35-42.

Yoshida S, Shiosaka S (1999) Plasticity-related serine proteases in the brain (review). Int J Mol Med 3: 405-9.

Yoshida S, Taniguchi M, Hirata A, Shiosaka S (1998) Sequence analysis and expression of human neuropsin cDNA and gene. Gene 213: 9-16.

Yoshioka A, Bacskai B, Pleasure D (1996) Pathophysiology of oligodendroglial excitotoxicity. J Neurosci Res 46: 427-37.

Yousef GM, Kishi T, Diamandis EP (2003) Role of kallikrein enzymes in the central nervous system. Clin Chim Acta 329: 1-8.

Figure legends

Figure 1

Expression of neuropsin mRNA in the spinal cord after crush injury. In situ hybridization was performed with a probe for neuropsin on cross sections immediately adjacent to the lesion. A, In untreated control mouse spinal cord, no neuropsin mRNA was found in the white matter, while a small number of cells in the gray matter expressed neuropsin mRNA. B, Neuropsin mRNA expression after SCI. Neuropsin mRNA expression at day 4 post-injury is shown. Neuropsin mRNA expression was induced in the white matter immediately adjacent to the lesion. C, Higher magnification of the boxed area in B. D, SCI-induced changes in neuropsin mRNA expression in the spinal cord. Levels of specific mRNA were measured by real-time PCR and normalized by the level of GAPDH mRNA expression in each individual sample. Each bar represents the mean ± SEM of 3 individual experiments. Statistical comparisons were made among all groups using raw data. Asterisks indicate significant differences from naive control (ANOVA with post hoc Fisher's PLSD test), $*P < 0.05$; $**P < 0.01$; $***P < 0.001$. Scale bars: C, 500 μm for A,B, 100 μm for C.

Figure 2

Improved functional recovery after crush SCI in neuropsin$^{-/-}$ mice. A, Time course of hindlimb locomotor performance in an open field over 14 days after SCI in WT and neuropsin$^{-/-}$ mice. WT mice (n = 12) exhibited the initial impairments of hindlimb performance after SCI that was gradually recovered over 14 days. Neuropsin$^{-/-}$ mice (n = 12) also showed the initial impairments of hindlimb performance followed by a gradual recovery, but the scores at day 10 and 14 was significantly higher than WT mice. B, Time course of rotorod performance over 14 days after crush SCI in WT and neuropsin$^{-/-}$ mice. Both strains of mice exhibited the initial impairments of rotorod performance followed by a gradual recovery, but neuropsin$^{-/-}$ mice showed a significantly improved performance at day 10 and 14. Asterisks indicate significant difference between WT and neuropsin$^{-/-}$ mice. (ANOVA with post hoc Fisher's PLSD test), $*P < 0.05$.

Figure 3

Attenuated demyelination in neuropsin$^{-/-}$ mice after crush SCI. A-D, Frozen cross sections of spinal cord from WT (A,C) and neuropsin$^{-/-}$ (B.D) mice at days 0 (A,B) and 14 (C,D) after SCI were processed for immunohistochemistry for MBP. Note the prominent defects in MBP immunoreactivity were obvious in WT mice at day 14 after SCI, whereas minimal demyelination was found in neuropsin$^{-/-}$ mice. E, Quantitative RT-PCR analysis for MBP mRNA expression. RNA from spinal cords of WT and neuropsin$^{-/-}$ mice at different time points after SCI was used to perform RT-PCR in a real-time LightCycler system. The level of each specific mRNA was measured by real-time PCR and normalized with the level of GAPDH mRNA expression in each individual sample. Each bar represents the mean ± SEM of 3 individual experiments after normalization with the level of naïve control. Statistical comparisons were made between WT and neuropsin$^{-/-}$ mice at each time point ($^*P < 0.05$, Student's t test). Scale bars: 100 μm for A-D.

Figure 4

Attenuated oligodendroglial cell death in neuropsin$^{-/-}$ mice after SCI. A, Using TUNEL, a significant number of cells showing DNA fragmentation were detected in the white matter of spinal cord sections from WT mice at day 1 and 4 (arrows). For the neuropsin$^{-/-}$ mice, significantly smaller number of TUNEL-positive cells were detected at days 1 and 4. B, The number of TUNEL-positive cells was counted in the white matter of the spinal cord within 400 μm rostral and caudal to the epicenter at different time points after SCI. Each bar represents the mean ± SEM of 3 individual experiments. Asterisks indicate significant differences between WT and neuropsin$^{-/-}$ mice (Student's t test), $^*P < 0.05$. C, Combined TUNEL and immunofluorescence for CNPase in the spinal cord of WT mice at day 4 after SCI. Most of the cells positive for TUNEL showed immunoreactivity for CNPase (arrows). Scale bars in A: 100 μm and C: 50 μm.

Figure 5

Attenuated oliodendroglial loss in neuropsin$^{-/-}$ mice after SCI. A-D, Spinal cord sections immediately adjacent to the lesion from WT (A,C) and neuropsin$^{-/-}$ (B,D)

mice at days 0 (A,B) and 14 (C,D) were processed for immunohistochemistry for CNPase. Extensive loss of CNPase-immunoreactive cells was obvious in WT mice at day 14 after SCI (C). For the neuropsin$^{-/-}$ mice, CNPase-immunoreactive cells were relatively preserved. E, The number of CNPase-immunoreactive cells was counted in spinal cord sections within 400 μm rostral and caudal to the epicenter from WT and neuropsin$^{-/-}$ mice at days 0 and 14 after SCI. Each bar represents the mean ± SEM of 3 individual experiments. Asterisks indicate significant differences between WT and neuropsin$^{-/-}$ mice (Student's *t* test), $*P < 0.05$. Scale bar: 100 μm for A-D.

Figure 6

Attenuated axonal damage and degeneration in neuropsin$^{-/-}$ mice after SCI. Frozen cross and section of the spinal from WT (A,B) and neuropsin$^{-/-}$ (C) mice of unlesioned control (A) and at day 14 after SCI (B,C) were processed for immunoreactivity for abnormally dephosphorylated NF-H. Note that WT mice had large amounts of abnormally dephosphorylated NF-H at day 14 after SCI (B) compared to neuropsin$^{-/-}$ mice (C).

Figure 7

Degeneration of axons was assessed by anterograde tract tracing with BDA. Horizontal sections of the spinal cord from WT (A-F) and neuropsin$^{-/-}$ (G-I) mice of unlesioned control (A-C) and at day 14 (D-I) after SCI were shown. B,C,E,F,H,I, Higher magnification images of respective boxed areas in A, D and G. In WT mice, decrease in the density of BDA-labeled CST fibers was seen rostral and caudal to the lesion site after SCI (D-F). Neuropsin$^{-/-}$ mice also showed axonal degeneration caudal but not rostral to the lesion (G-I). Arrows in I indicate surviving axons cauldal to the lesion. The injury site is indicated with arrowheads. J, The number of CST fibers 1.0 mm rostral and caudal to the epicenter at days 0 and 14 after SCI. Each bar represents the mean ± SEM of 3 individual experiments. Asterisks at each bar indicate significant differences from respective naïve controls ($*P < 0.05$; $**P < 0.01$; $***P < 0.001$, Student's *t* test). Statistical comparisons were also made between WT and neuropsin$^{-/-}$ mice in each condition ($**P < 0.01$, Student's *t* test). Scale bar in I:

500 μm for A,D,G and 100 μm for B,C,E,F,H,I.

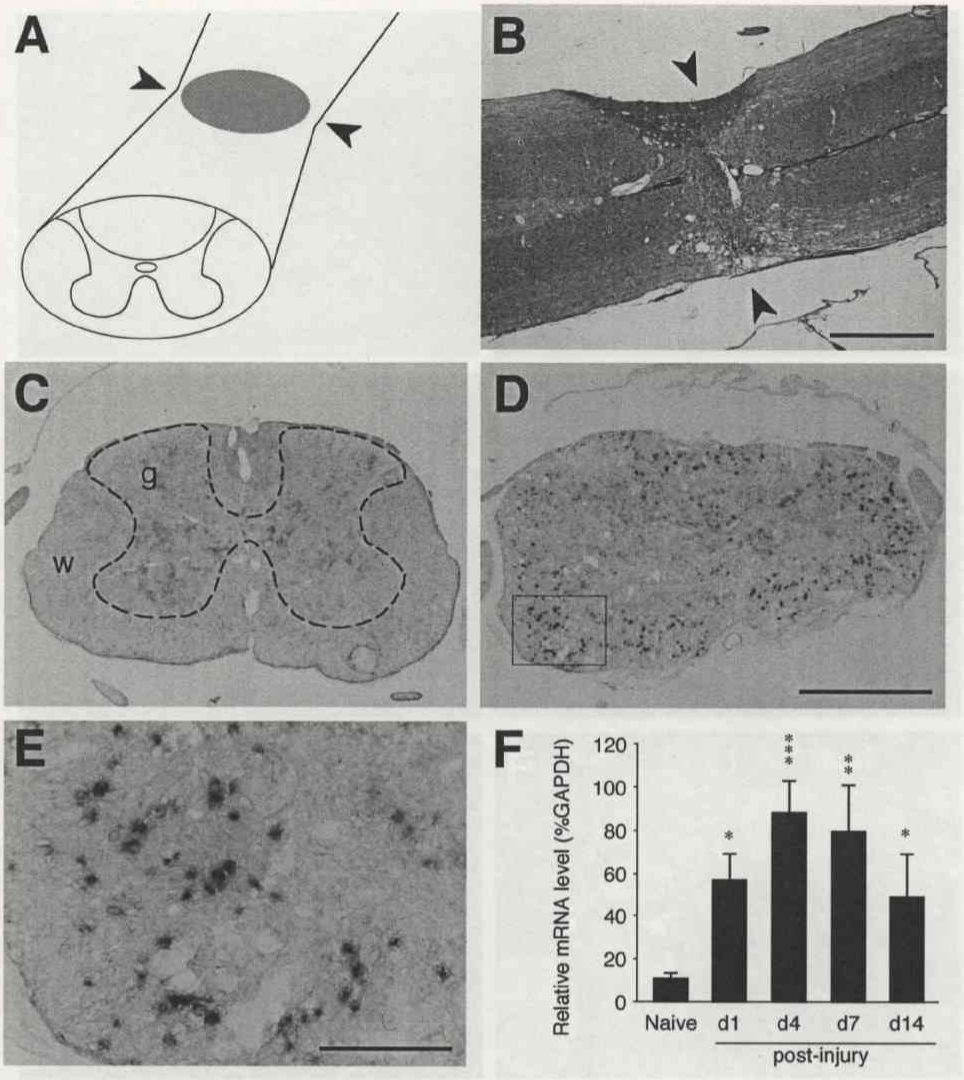
A
B
C
g
w
D
E
F
Relative mRNA level (%GAPDH)
120
100
80
60
40
20
0
***
**
*
*
Naive
d1
d4
d7
d14
post-injury

Fig. 1

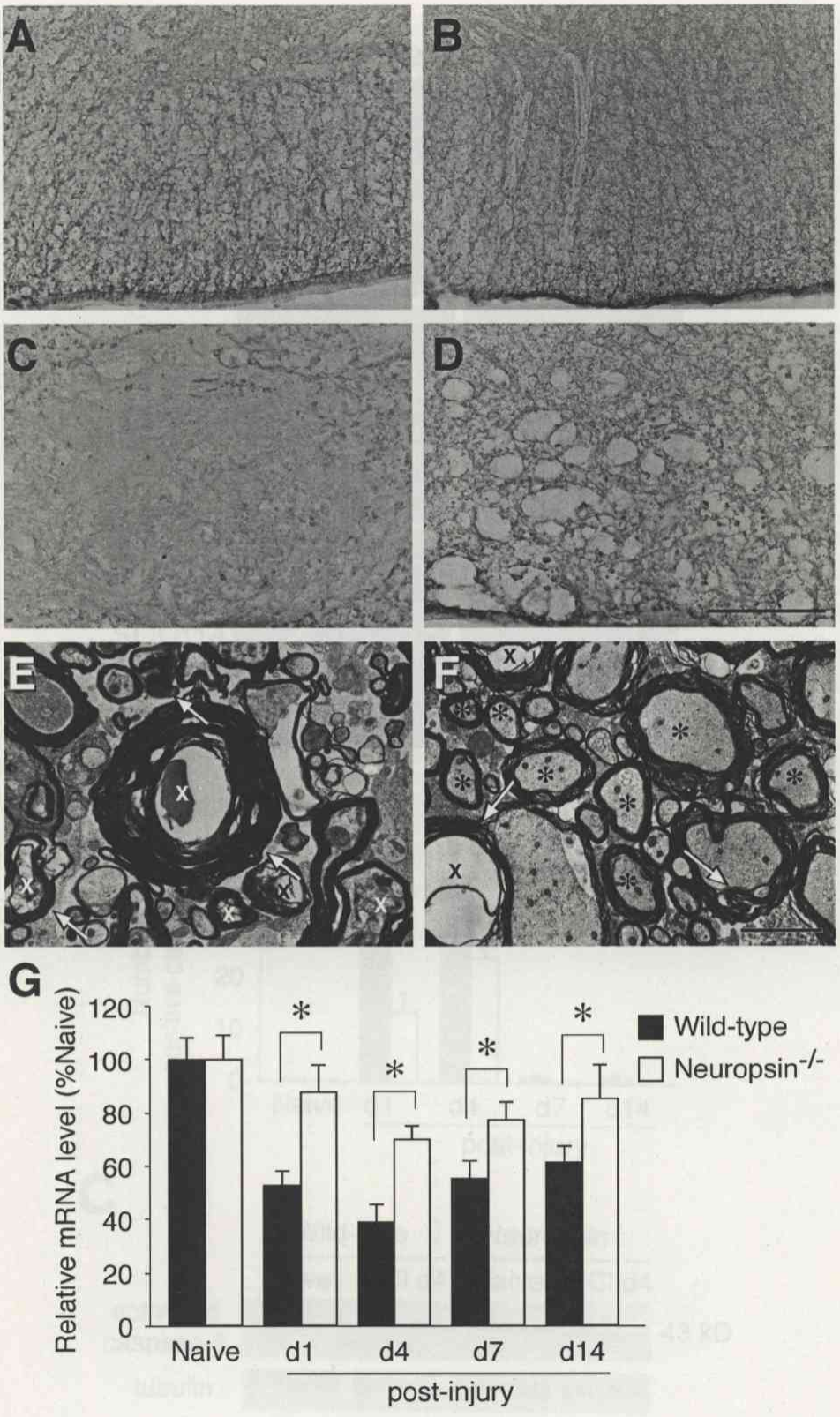
A
B
C
D
E
F
G
Relative mRNA level (%Naive)
120
100
80
60
40
20
0
Naive
d1
d4
d7
d14
post-injury
Wild-type
Neuropsin-/-
*

Fig. 2

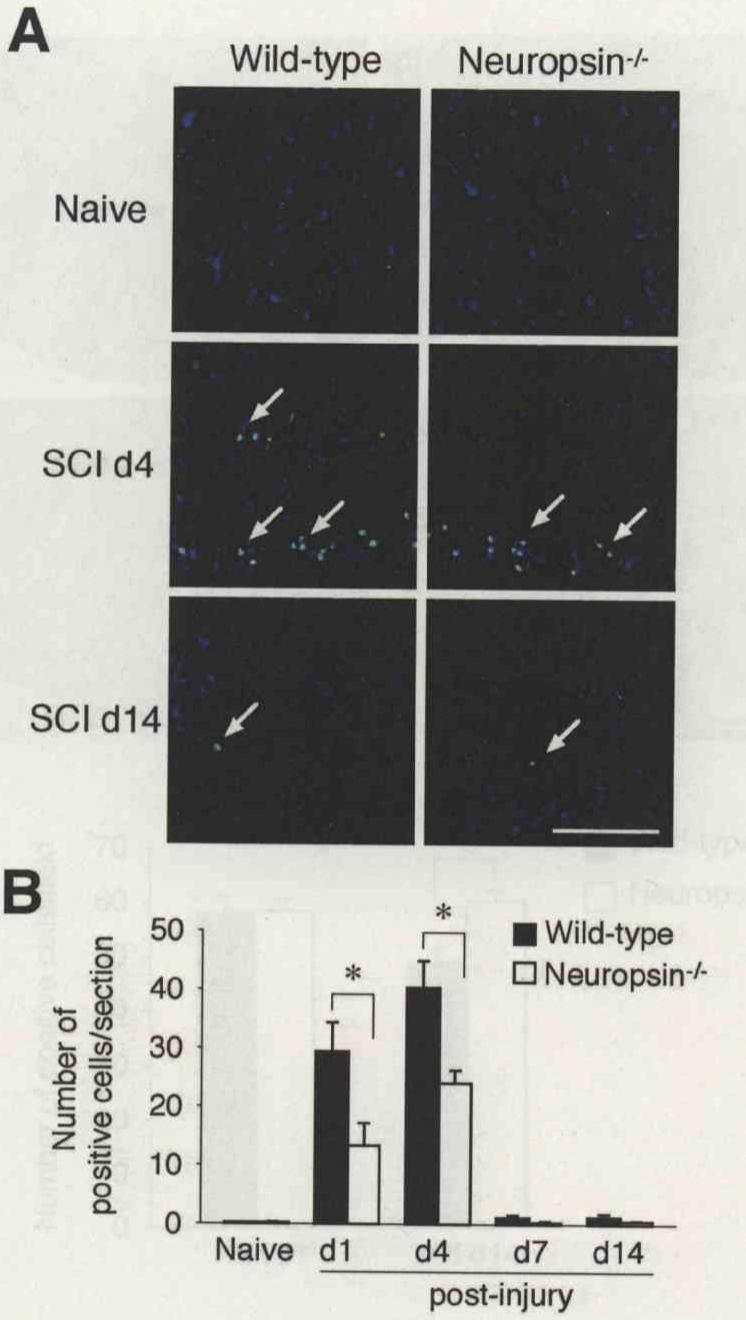
A
Wild-type
Neuropsin-/-
Naive
SCI d4
SCI d14
B
Number of positive cells/section
50
40
30
20
10
0
*
*
Wild-type
Neuropsin-/-
Naive
d1
d4
d7
d14
post-injury
C
Wild-type
Neuropsin-/-
Naive
SCI d4
Naive
SCI d4
activated caspase-3
43 kD
tubulin

Fig. 3

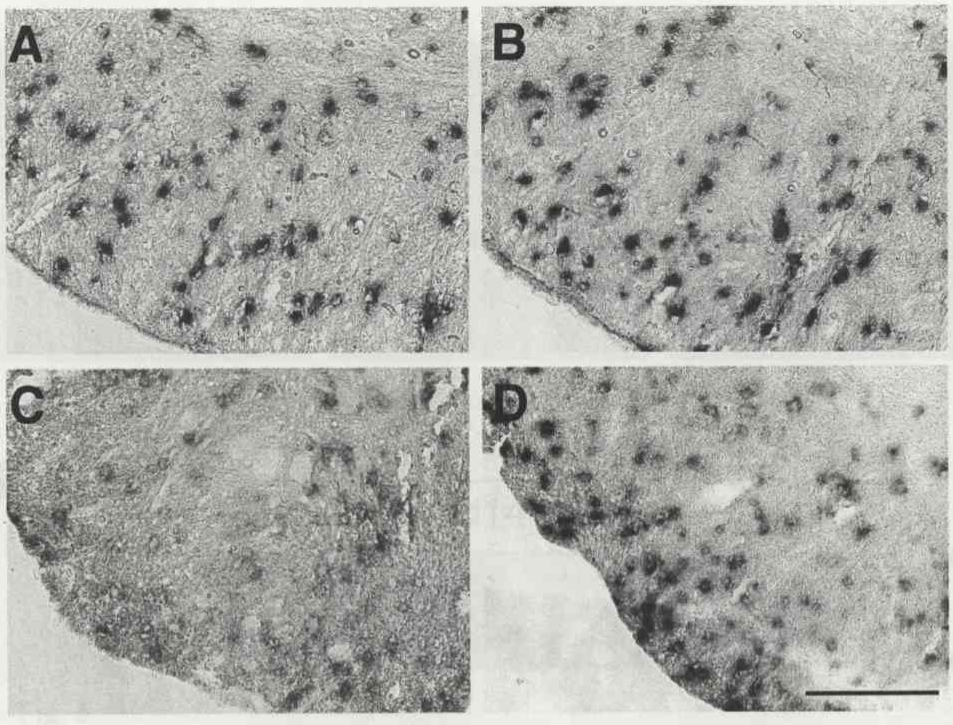
A
B
C
D

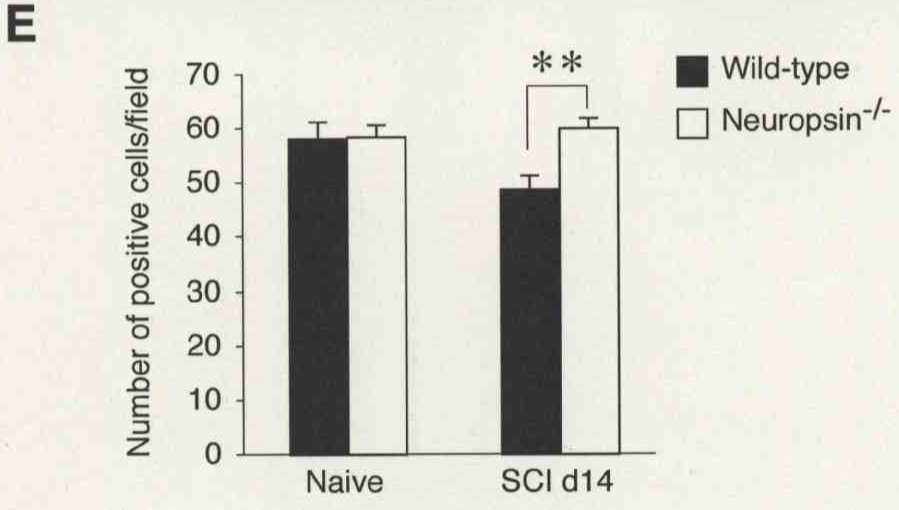
E
Number of positive cells/field
70
60
50
40
30
20
10
0
**
Wild-type
Neuropsin-/-
Naive
SCI d14

Fig. 4

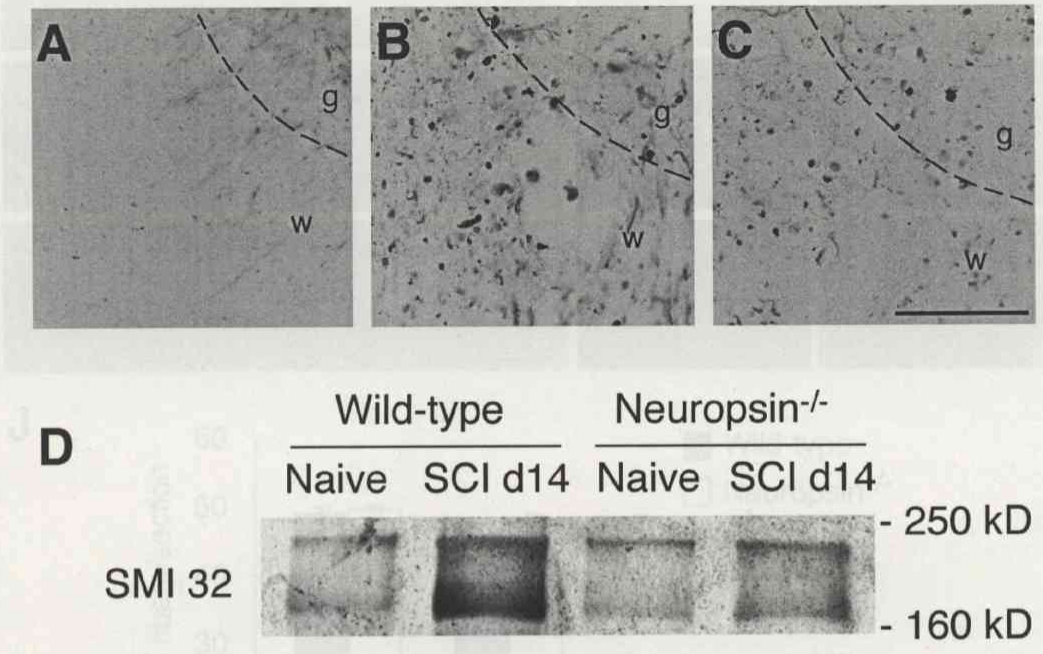
A
g
w
B
g
w
C
g
w
D
Wild-type
Neuropsin-/-
Naive
SCI d14
Naive
SCI d14
SMI 32
- 250 kD
- 160 kD

Fig. 5

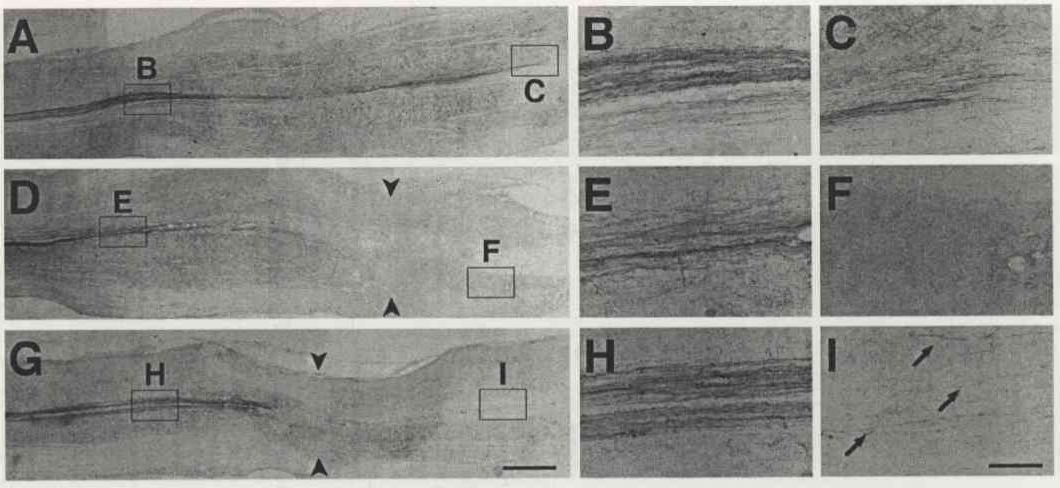
A
B
C
D
E
F
G
H
I
B
C
E
F
H
I

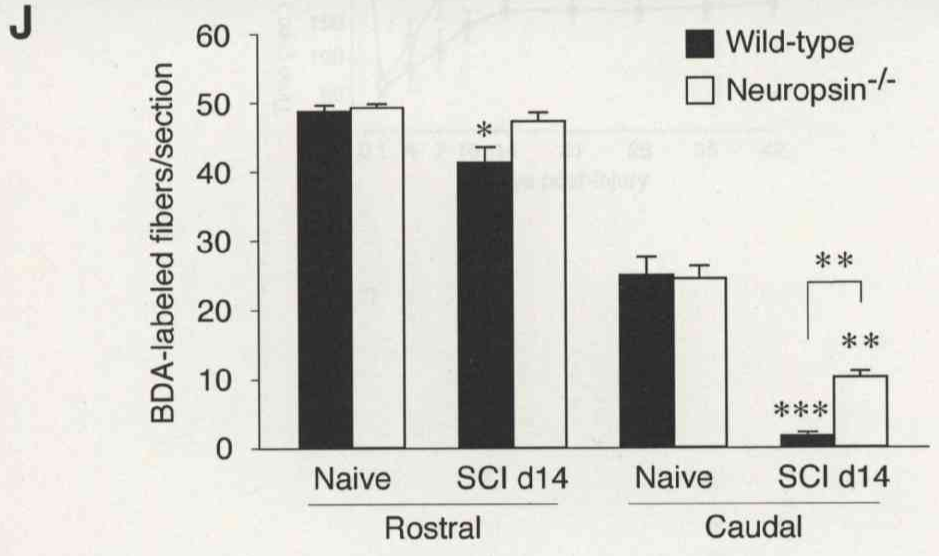
J
BDA-labeled fibers/section
60
50
40
30
20
10
0
Wild-type
Neuropsin-/-
*
**
**
***
Naive
SCI d14
Naive
SCI d14
Rostral
Caudal

Fig. 6

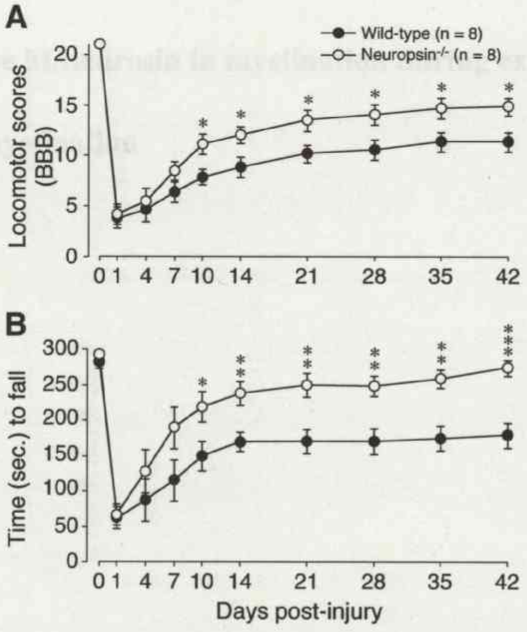
A
Wild-type (n = 8)
Neuropsin-/- (n = 8)
Locomotor scores (BBB)
20
15
10
5
0
0 1 4 7 10 14 21 28 35 42
B
Time (sec.) to fall
300
250
200
150
100
50
0
0 1 4 7 10 14 21 28 35 42
Days post-injury

Fig. 7